Lithium-antimony-lead liquid metal battery for grid-level storage

Kangli Wang, Kai Jiang, Brice Chung, Takanari Ouchi, Paul J. Burke, Dane A. Boysen, David J. Bradwell, Hojong Kim, Ulrich Muecke, and Donald R. Sadoway*

Affiliations:

Department of Materials Science and Engineering, Massachusetts Institute of Technology, 77 Massachusetts Avenue, Cambridge, Massachusetts 02139-4307, United States of America

Abstract:

Energy storage on the electric grid would greatly improve efficiency and reliability while enabling integration of intermittent renewable energy technologies, e.g., wind and solar, into baseload[1-4]. In this regard, batteries have long been considered strong candidate solutions due to their small footprint, mechanical simplicity, and flexibility in siting. However, the barrier to widespread adoption of batteries is their high cost. Herein we disclose a Li||Sb-Pb liquid metal battery that meets the performance specifications for stationary energy storage applications. The battery comprises a liquid lithium negative electrode, a molten salt electrolyte, and a liquid antimony-lead alloy positive electrode, which self-segregate by density into three distinct layers owing to the immiscibility of the contiguous salt and metal phases. The all-liquid construction confers the advantages of higher current density, longer cycle life, and simpler manufacturing of large-scale storage systems (no membranes or separators) compared to those of conventional batteries[5,6]. At charge-discharge current densities of 275 mA cm^{-2} the cells cycled at 450°C with 98% coulombic efficiency and 73% round-trip energy efficiency. As evidence of their high power capability the cells were discharged and charged at current densities as high as 1000 mA cm^{-2}. Measured capacity loss after 1800 h operation (more than 450 charge-discharge cycles at 100% depth of discharge) projects retention of over 85% of initial capacity after 10 years of daily cycling. Our results demonstrate that alloying a high-melting and high-voltage metal (Sb) with a low-melting and low-cost metal (Pb)

advantageously decreases the operating temperature while maintaining a high cell voltage. Apart from the fact that this finding puts us on a desirable cost trajectory, this approach may well be more broadly applicable to other chemistries.

Main Text:

Among metalloids and semi-metals, Sb stands as a promising positive electrode candidate for its low cost ($1.23 mol^{-1}) and relatively high cell voltage when coupled with an alkali or alkaline-earth negative electrode[5]. In previous work[6], we demonstrated the performance of a Mg||Sb liquid metal battery at current rates ranging from 50 to 200 mA cm^{-2}, achieving up to 69% round-trip energy efficiency. However, the high melting points of Mg (T_m = 650°C) and Sb (T_m = 631°C) require the cell to operate near 700°C. From a system's perspective a high operating temperature is undesirable as it results in elevated rates of corrosion and detracts from overall storage efficiency, which ultimately increases cost of ownership. These potential limitations in conjunction with an estimated electrode materials cost of $375/kWh and average cell voltage of 0.21 V (measured under galvanostatic discharge at 200 mA cm^{-2}) render Mg||Sb cells impractical for commercial applications[5].

With an average cell voltage of 0.92 V, the Li||Sb couple is an appealing alternative[7]. Moreover, Li melts at 180°C and exhibits a low solubility in lithium halide melts, which results in lower self-discharge current and hence higher energy efficiency especially when compared to sodium alternatives[8]. Despite these attractive properties, the high melting point of Sb sets the operating temperature of the Li||Sb cell at almost 500°C above the melting point of Li. While alloying Sb with another metal can be an effective strategy to lower the melting point of the positive electrode, this is generally accompanied by an undesirable decrease in cell voltage, as observed in the Mg||Sn-Sb[9] and Na||Bi-Sb systems[10].

Herein, with the use of a Li anode, we discovered that the addition of Pb to Sb maintains a near-pure Sb-like high cell voltage while substantially reducing the melting temperature (eutectic composition Sb-Pb 18-82 mol%, melting temperature T_m = 253°C[11]). Figure 1 shows the equilibrium voltage of the Li||Sb-Pb cell as a function of Li

concentration in various Sb-Pb alloys. Measurements were made by coulometric titration in a LiF-LiCl-LiI molten salt electrolyte (20-50-30 mol%, T_m = 430°C). Four compositions of Sb-Pb alloys are shown here: 50-50, 40-60, 30-70, and 18-82 mol% (eutectic composition). The corresponding equilibrium voltages of the binary Li||Sb cell[12] and the binary Li||Pb cell[13] are also shown for comparison. At the chosen experimental temperature (450°C), Sb-Pb alloys and pure Pb are liquid, whereas Sb is solid. As shown in Fig. 1, the Li||Sb (solid) chemistry has the highest cell voltage at 0.92 V, while the Li||Pb chemistry exhibits the lowest cell voltage, just under 0.6 V. Interestingly, even at high dilution (up to 82 mol% Pb in Sb), the Li||Sb-Pb systems operate at cell voltages very near Li||Sb-like levels (only about 0.05 V lower), indicating that the Li-Sb-Pb electrode potential is determined primarily by the Li-Sb interaction. In order to reveal the predominant role of Sb in setting the potential, Figure 1a was normalized to the concentration of Li relative to Sb. Figure 1b shows that all Li-Sb-Pb electrodes share a behavior similar to that of the Li-Sb electrode: in each case, a near-constant high-potential region followed by a drop in potential at 75 mol% Li relative to Sb. This behavior is suggestive of the Li||Sb system in which Li_xSb ($x < 3$) compounds are formed and thereby generate a high electrode potential versus pure Li. When the concentration of the alloy reaches 75 mol% Li in Sb, a low-potential Li_3Sb phase is formed, and the cell voltage drops precipitously[7].

Cell performance was demonstrated in 1.9 Ah theoretical capacity cells (3.16 cm^2 positive electrode/electrolyte interfacial area) fitted with a Li negative electrode, an Sb-Pb positive electrode (30-70 mol%), and a LiF-LiCl-LiI molten salt electrolyte (20-50-30 mol%, T_m = 430°C). Cells were assembled in the fully charged state in an argon-filled glove box, placed inside a sealed test vessel, and operated in a vertical tube furnace at 450°C. When the temperature exceeded the melting point of the salt, the equilibrium cell voltage stabilized at ~1.0 V, consistent with titration results. At a stepped-potential of 1.2 V the self-discharge current was measured to be 0.6 mA cm^{-2}, which is significantly lower than the value observed in Na systems (20 mA cm^{-2})[8]. This is attributable to the lower solubility of Li in its molten halides[14]. A typical charge/discharge voltage profile and the usual performance metrics as a function of cycle index are shown in Figure 2. At

a high current rate of 275 mA cm^{-2}, cells consistently achieved on average 93% of theoretical capacity, demonstrating the facile electrode kinetics and favorable transport properties of liquid metal batteries. The nominal discharge voltage was 0.73 V, more than 3 times higher than that of Mg||Sb. Based on the measured cell performance, the electrode materials costs are estimated to be $68/kWh, about one fifth of the comparable value for Mg||Sb cells.

For stationary applications, long service lifetime is a critical factor. Liquid metal batteries are advantageous owing to the liquid electrodes and molten salt electrolyte, which avoid many of the common failure mechanisms associated with batteries fitted with solid-state electrodes, e.g., undesirable film formation at the electrode/electrolyte interface, or phase transformations that mechanically damage cell components[15]. Here we show the results of charge/discharge cycle testing of the Li||Sb-Pb system (Figure 2b). Over the duration of the test, the cells exhibited a coulombic efficiency of 98% and a round-trip energy efficiency of 73%, maintaining 94% of the initial capacity after 450 cycles at full depth of discharge. The capacity fade rate decreased after the 100^{th} cycle whereupon the fade rate between 100^{th} to 450^{th} cycles was 0.004 % $cycle^{-1}$. This is tantamount to retention of over 85% of initial capacity after 10 years of daily cycling. Cross-sections of cells after 1800 h of operation did not exhibit any obvious corrosion of cell components (current collectors and walls).

The ability to operate at high current densities with minimal impact on cycle life is an asset for certain grid applications such as ancillary services. Here, we show the capability of Li||Sb-Pb cells with LiF-LiCl-LiI salt electrolyte (20-50-30 mol%, T_m = 430°C) operating at current densities as high as 1000 mA cm^{-2} (Figure 3) not only while discharging, but also while charging, the latter especially useful for such applications as frequency regulation. At current densities as high as 500 mA cm^{-2}, there is no significant decrease of the reversible capacity (87% of theoretical value). Even at the highest current density (1000 mA cm^{-2}), the cell performed at 54% of theoretical capacity. Most noteworthy about this last observation is the ability of the cell to act as a high-current load without incurring permanent damage: efficiency in this instance is subordinate to long-term electrode stability. This advantageous mix of features is attributable to the rare

combination of high conductivity of the molten salt electrolyte, ultrafast charge-transfer kinetics at the electrode-electrolyte interface between liquid metal and molten salt, and fast mass transport within liquid metal electrodes.

To demonstrate the scalability of the system, 62 Ah theoretical capacity (62 cm^2) cells were constructed and operated with performance similar to that achieved at small scale (1.9 Ah). To optimize systems costs, a LiF-LiCl-LiBr eutectic electrolyte (22-31-47, T_m = 443°C) and a positive electrode Sb-Pb composition of 40-60 mol% were chosen. Operating at a temperature of 500°C cells were cycled at 275 mA cm^{-2}. Figure 4 shows a typical charge/discharge voltage profile and the cell performance metrics over twenty cycles. With average values of coulombic efficiency of 98% and round-trip energy efficiency of 71%, negligible capacity fade was observed over the duration of the test. The nominal discharge voltage was measured to be ~0.69 V. On this basis, the electrode materials costs were estimated to be $65/kWh.

In summary, alloying Sb with Pb has been identified as a way to achieve significant reductions in melting point of the positive electrode as well as cell operating temperature without an attendant decrease in cell voltage. This finding not only lowers the cost of Li||Sb-Pb batteries increasing their attractiveness for stationary applications, but also serves as an example of how to broaden the selection of positive electrode materials for liquid metal batteries. [–]

Methods:

For all experiments, high purity (> 99.9%) and ultra-dry grade LiF, LiCl, LiBr, and LiI salts (Alfa Aesar) were used in electrolytes. Salt mixtures were dried under vacuum at 80°C for 8 h and 250°C for 2 h to remove residual water and then melted under argon gas at 600°C. All experiments were performed under a high purity argon atmosphere.

For the evaluation of equilibrium voltage by coulometric titration, all alloys target compositions were prepared using an arc-melter (MAM1, Edmund Bühler GmbH). After arc-melting, alloys were placed into a small mullite basket, pre-melted and used as working electrodes. Electrical contact was established using a tungsten wire (1 mm

diameter) immersed in the Sb-Pb alloy. An Ag/AgCl served as the reference electrode (3 wt% AgCl in LiCl-NaCl-KCl eutectic mixture) and contained within a closed-end mullite tube with the end polished to a thin micro-porous layer. A 40-60 mol% Li-Al alloy was used as the counter electrode. Electrochemical measurements were performed with an Autolab PGSTAT 302N potentiostat/galvanostat.

For cell testing, galvanostatic charge and discharge were performed using an Arbin BT2000. Alloys were pre-weighed and placed in cell containers. The salt mixtures were introduced and dried in-situ under vacuum at 80°C for 8 h and 250°C for 4 h before setting the operating temperature for electrochemical testing.

All electrode cost estimations were performed using the following formula: $= (\sum_i P_i . m_i)/E$, where C is the capital cost per unit of discharged electrical energy in US \$ kWh^{-1}, P_i is the specific bulk metal cost in \$ kg^{-1}, m_i is the metal's mass in kg, and E is the discharged energy in kWh. For Li||Sb-Pb cells, the value of discharged energy, E, was that measured during galvanostatic cycling at 275 mA cm^{-2} (Fig. 2 and Fig. 4). For Mg||Sb cells, the discharged energy, E, was that measured during galvanostatic cycling at 200 mA cm^{-2} [6]. Average bulk metals prices of lithium (61.7 \$ kg^{-1}), magnesium (2.7 \$ kg^{-1}), lead (2.1 \$ kg^{-1}), and antimony (10.1 \$ kg^{-1}) were obtained from the literature[16]. Balance of system and salt costs were not included as the technology has yet to be fully developed at commercial scale, so there is no accurate basis for such estimation.

Extended data:

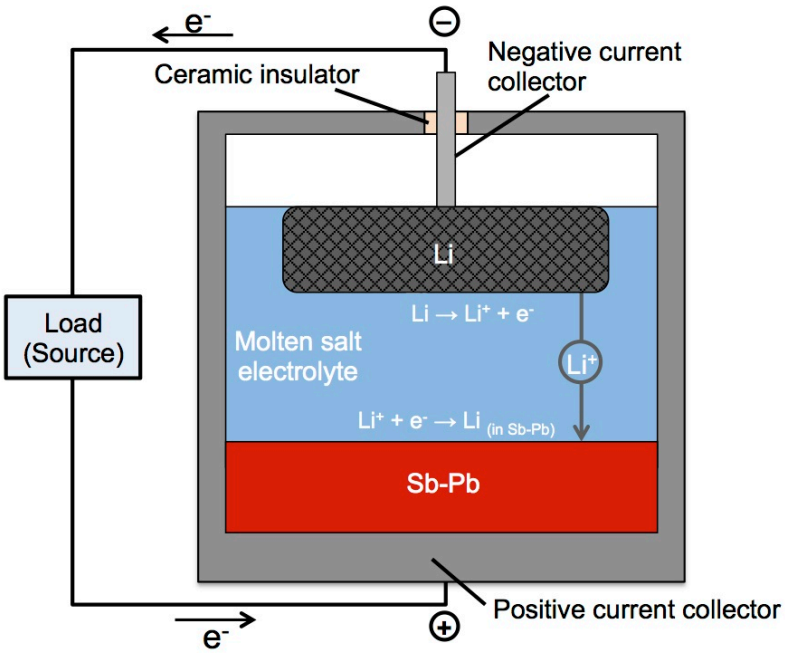

Extended Data Figure 1 | Cell schematic of Li||Sb-Pb liquid metal battery. The negative current collector consists of a stainless steel rod and Fe-Ni foam. The positive current collector is made of graphite (small cell, 3.16 cm^2 active area) or 304 stainless steel (large cell)., 62 cm^2 active area). Current collectors are electrically isolated by means of an alumina insulator.

References and Notes:

1. G.L. Soloveichik, Battery technologies for large-scale stationary energy storage. *Ann. Rev. Chem. Biomol. Eng.* **2**, 503-527 (2011).
2. B. Dunn, H. Kamath, J.-M. Tarascon. Electrical energy storage for the grid: a battery of choices, *Science* **334** (6058), 928-935 (2011).
3. Z. Yang et al. Electrochemical energy storage for green grid. *Chem. Rev.* **111**, 3577-3613 (2011).
4. C.J. Barnhart, S.M. Benson. On the importance of reducing the energetic and material demands of electrical energy storage. *Energy Environ. Sci*. **6**, 1083-1092 (2013).

5. H. Kim et al. Liquid metal batteries: past, present, and future. *Chem. Rev.* **113**, 2075-2099 (2013).

6. D.J. Bradwell, H. Kim, A.H.C. Sirk, D.R. Sadoway, Magnesium-antimony liquid metal battery for stationary energy storage. *J. Am. Chem. Soc*., **134**, 1895-1897 (2012).
7. W. Weppner, R.A. Huggins. Thermodynamic properties of the intermetallic systems lithium-antimony and lithium-bismuth. *J. Electrochem. Soc*. **125**, 7-14 (1978).
8. E.J. Cairns, C.E. Crouthamel, A.K. Fischer, M.S. Foster, J.C. Hesson. Galvanic cells with fused salts, *ANL-7316; Argonne National Laboratory* (1967).
9. C.A. Eckert, R.B. Irwin, J.S. Smith. Thermodynamic activity of magnesium in several highly-solvating liquid alloys. *Metall. Trans. B*. **14**, 451-458 (1983).
10. A.G. Morachevskii, E.V. Bochagina, M.A. Bykova. Thermodynamic properties of bismuth-sodium-antimony liquid alloys. *Zh. Prikl. Khim.* **73**, 1620-1624 (2011).
11. H. Ohtani, K. Okuda, and K. Ishida. Thermodynamic study of phase equilibria in the Pb-Sn-Sb System. *J. Phase Equilib.*, **16**, 416-429 (1995).
12. A.G. Morachevskii. Thermodynamic analysis of alloys of the lithium-antimony system. *Zh. Prikl. Khim*., **75**, 367-369 (2002).
13. W. Gasior, Z. Moser. Thermodynamic study of lithium-lead alloys using the EMF method. *J. Nucl. Mater.* **294**, 77-83 (2001).
14. A.S. Dworkin, H.R. Bronstein, M.A. Bredig. Miscibility of metals with salts. VI. Lithium-lithium halide systems. *J. Phys. Chem.* **66**, 572-573 (1962).
15. L. S. Kanevskii and V. S. Dubasova. Degradation of Lithium-Ion Batteries and How to Fight It: A Review. Russ. J. Electrochem. **41**(1), 1–16 (2005), translated from Elektrokhimiya, **41**(1), 3–19 (2005).
16. MetalPrices Online Database. http://www.metalprices.com.

Acknowledgments:

Financial support from the Advanced Research Projects Agency-Energy (U.S. Department of Energy) and Total, S.A. is gratefully acknowledged.

Author Contributions:

K.W. conducted equilibrium voltages measurements. K.W., K.J., T.O., D.J.B., and U.M. performed small scale cell testing. B.C and P.J.B performed cell testing at engineering scale. D.R.S., D.A.B., and H.K. conceived the project. K.W., K.J., B.C., T.O., and D.R.S. drafted the manuscript.

Author Information:

Reprints and permissions information is available at www.nature.com/reprints. The authors declare no competing financial interests. Readers are welcome to comment on the online version of the paper. Correspondence and requests for materials should be addressed to D.R.S. (dsadoway@mit.edu).

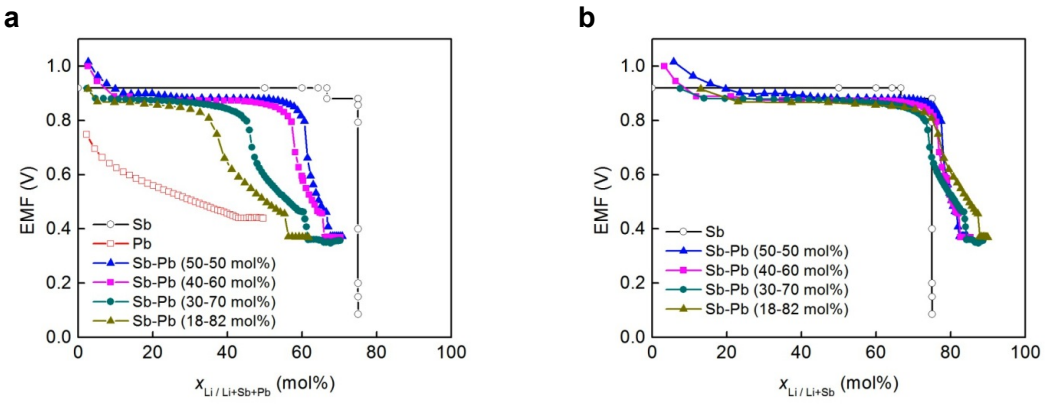

Figure 1 | Open circuit potentials (OCPs) of Li-Sb-Pb electrodes vs Li/Li$^+$ measured by coulometric titration at 450°C. (**a**) as a function of Li concentration in Sb-Pb alloys, and (**b**) as a function of Li concentration normalized with respect to Sb. Pure Sb data from ref. 7.

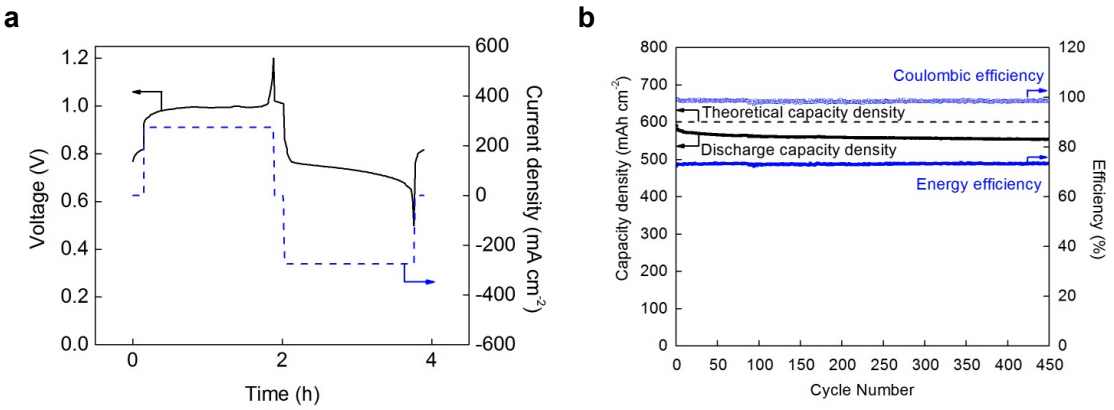

Figure 2 | Performance of a Li||Sb-Pb cell cycled at 275 mA cm^{-2}. (**a**) profile of voltage and current density during charge/discharge (15th cycle), (**b**) coulombic efficiency, energy efficiency, and discharge capacity density as a function of cycle number. Theoretical cell capacity was 1.9 Ah with a fully discharged target composition of 45% Li in an $Sb_{30\%}$-$Pb_{70\%}$ alloy (3.16 cm^2 of active surface area). Operating temperature was 450°C.

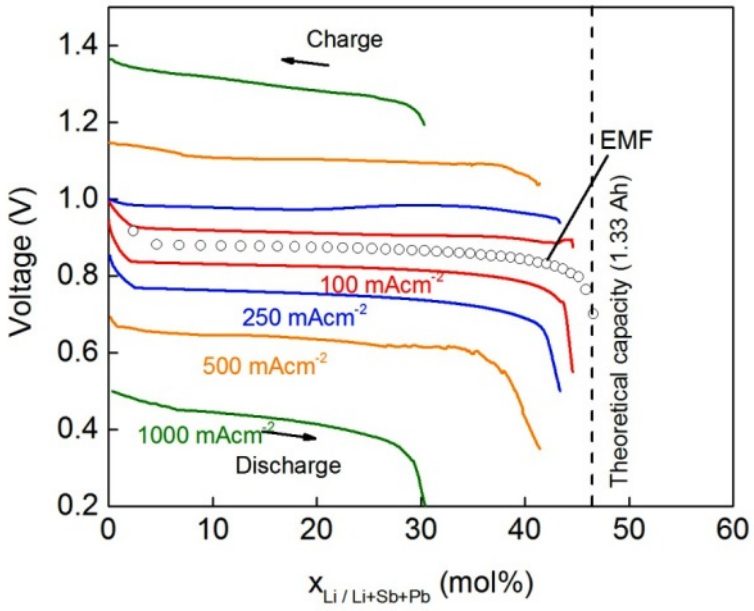

Figure 3 | Voltage profiles during charge/discharge at different current densities (100-1000 mA cm^{-2}) of a Li||Sb-Pb cell. Theoretical capacity was 1.33 Ah with a fully discharged target composition of 45% Li in a $Sb_{30\%}$-$Pb_{70\%}$ alloy (2.0 cm^2 of active surface area). Operating temperature was 450°C.

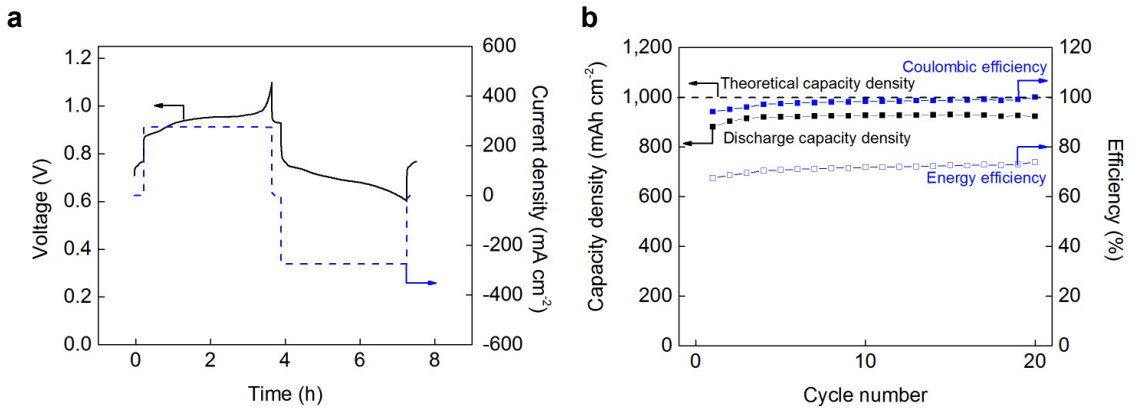

Figure 4 | Performance of a Li||Sb-Pb cell cycled at 275 mA cm^{-2}. (**a**) profile of voltage and current density during charge/discharge (15th cycle), (**b**) coulombic efficiency, energy efficiency, and discharge capacity density as a function of cycle number. Theoretical cell capacity was 62 Ah with a fully discharged target composition of 52.4% Li in a $Sb_{40\%}$-$Pb_{60\%}$ alloy (62 cm^2 of active surface area). Operating temperature was 500°C.